ACS OMEGA

Open Access

http://pubs.acs.org/journal/acsodf

Article

Exposure of Polystyrene Micro- and Nanoplastics to Simulated Human Digestive Enzymatic Systems: Structural and Functional Implications

Ananthaselvam Azhagesan and Natarajan Chandrasekaran*

Cite This: *ACS Omega* 2025, 10, 10866−10877

Read Online

ACCESS | Metrics & More | Article Recommendations | Supporting Information

ABSTRACT: The current in vitro study explores the exposure of the emerging pollutants polystyrene micro- and nanoplastics (PS-MNPs) within the digestive system and their interaction with key digestive enzymes such as α-amylase, pepsin, and pancreatin. The present research aims to elucidate the potential health implications of digestive enzymes by PS-MNPs based on the previously estimated mean of ingested microplastics (MPs) (0.714 g/day). The study deepens our understanding of the environmental pollutants' impact on human health by examining the interactions between polystyrene (PS) microplastics (PS MPs, 37−50 μm approx.) and PS nanoplastics (PS NPs, 100 nm) with digestive enzymes. The study analyzes the effects of micro- and nanosized plastics on enzyme activity using multiple spectroscopic techniques, revealing the molecular mechanisms of enzyme inhibition and structural changes caused by PS NPs, more than those by PS MPs. The fluorescence emission spectra indicated a static quenching mechanism across all the digestive enzymes at K_q = 3.638, 4.615, and 1.855 ($\sim\times 10^{18}$ $M^{-1}\cdot s^{-1}$), predominantly affecting tyrosine (Tyr) and tryptophan (Trp) residues. Resonance light scattering (RLS) spectra confirmed the formation of enzyme−PS NPs complexes, leading to aggregation. Fourier transform infrared (FT-IR) and circular dichroism (CD) spectrometry results showed a decrease in protein content and structural alterations in the enzymes, potentially affecting their function. The half inhibitory concentration (IC_{50}) values of PS NPs for salivary α-amylase (180 μg/mL), pepsin (580 μg/mL), and pancreatic protease (314 μg/mL) indicate uncompetitive inhibition, and that of pancreatic α-amylase (592 μg/mL) indicates mixed reversible inhibition of digestive enzymes. The study highlights the potential health risks associated with PS NPs exposure and gives a broader understanding of the interplay between environmental plastic pollutants and human health.

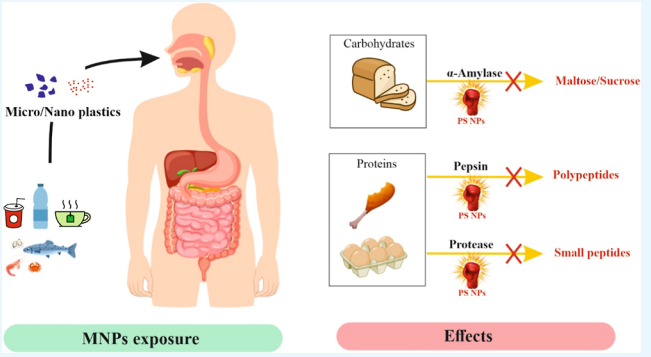

1. INTRODUCTION

Plastic pollution has become a global crisis escalating in both scale and severity.[1] It encompasses a variety of aspects from sourcing raw materials for plastic production to managing the disposal of extensive plastic waste.[2] The adverse effects of plastic pollution extend across environmental ecosystems, impacting the animal health.[3] Moreover, there are potential implications for human well-being too.[4] Primary microplastics (MPs) are deliberately manufactured for consumer and industrial purposes, and secondary MPs are formed from the degradation of larger plastic items contributing to the environmental crisis.[5,6] Their sources are diverse, comprising smaller materials originating from the breakdown of larger plastic items, synthetic textiles, and industrial processes.[7] These tiny particles can be found in soil and water bodies and even exist in the air we inhale.[4,8] These minuscule plastic particles can travel long distances due to their lightweight and inert properties.[9]

Plastics have far-reaching impacts on daily life, including technology, medicine, and domestic use.[17] Unfortunately, most people discard plastics after a single use, causing environmental challenges as they accumulate in landfills, oceans, and waterways.[2] The breakdown of plastics into micro- and nanoplastics (MNPs) raises concerns about their toxicity to both the environment and humans.[5,18] As they persist in the environment, humans encounter MPs through various pathways including ingestion, inhalation, and skin contact.[10,11] Recent scientific findings have detected MPs in human biological samples including excrement, biofluids, and tissues.[12,13] Toxicological research indicates that MPs can disrupt energy balance, alter intestinal microflora, and affect the reproductive, immune, and nervous systems.[14]

Received: August 30, 2024
Revised: February 11, 2025
Accepted: February 13, 2025
Published: March 11, 2025

Although previous research has examined the environmental effects of MNPs, there is still limited understanding of their impact at the subcellular or molecular levels within the human body.[15] Furthermore, MPs may enhance the toxicity of other environmental pollutants.[16] For instance, refs 17 and 18 have reported the long-time exposure of polystyrene nanoplastics (PS NPs) to fish models, illustrating the inhibition of digestive enzymes in *Epinephelus coioides* and *Larimichthys polyactis*. Despite some research carried out on the risks posed by MPs to human health, the exploration of individual digestive enzymatic systems remains in its early stages, leaving many questions unanswered.

Digestive enzymes play a critical role in maintaining human health. The salivary gland secretes α-amylase, which is released into the mouth for the hydrolysis of carbohydrate polysaccharides into monosaccharides.[19] Pepsin, an enzyme found in gastric juice, is essential for protein hydrolysis, breaking down proteins into smaller polypeptide units.[20] Pancreatin, a combination of digestive enzymes (including α-amylase, protease, and lipase), is produced by the exocrine cells of the pancreas. α-Amylase hydrolyzes carbohydrates, protease digests proteins, and lipase breaks down fats.[21] These processes from the digestive system enable the human body to extract essential nutrients.

Research carried out on the effects of MNPs on digestive enzymes has been limited. Earlier studies have suggested that an increase in PS concentration can inhibit lipase activity, thereby slowing down the digestion process facilitated by the lipase enzyme.[22] Additionally, an increase in the concentration of PS nanoparticles has been linked to the inhibition of human salivary α-amylase enzyme activity.[23] So, it is necessary to investigate the interaction of NPs traversing the digestive system causing systemic exposure. The survey on previous studies inspires future work on exploring MNPs creation and their behavior within the environment, toxicity levels, pollution, and potential health impacts on human.

Based on the knowledge obtained from the previous studies, this study focuses on the individual digestive systematic enzyme response of PS-MNPs. The study is crucial for addressing the emerging environmental and health challenges. In our present work, the interaction of micro- and nano-polystyrene (PS-MNPs) inhibiting the three crucial digestive enzymes α-amylase, pepsin, and pancreatin (protease and α-amylase) was investigated. Our methodology integrates in vitro experiments including fluorescence spectroscopy, Fourier transform infrared (FT-IR) spectroscopy, enzyme inhibition assays, and inhibition-type studies to investigate the impact of plastics within the complex microenvironment of the human digestive system.

2. MATERIALS AND METHODS

2.1. Chemical and Reagents. Nonfunctionalized PS NPs $(C_8H_8)_n$ of size: 100 nm (Cat. No: 00876-15) and PS (MW 50,000) (Cat. No: 18544-100) were purchased from Polysciences, Inc., Warrington, United States. (The prepared PS particle sizes were characterized and are represented in Supporting Information Figure S1). The human salivary α-amylase (Type-XIII-A) (A1031) (EC 3.2.1.1), pepsin from porcine pancreas (EC 3.4.23.1) (Cat. No: P7012), pancreatin from porcine (Cat. No: P7545), hemoglobin porcine (Cat. No: H4131), casein from bovine milk (Cat. No: C7078), and potassium phosphate (dibasic trihydrate) (Cat. No: P5504) were purchased from Sigma-Aldrich, Bangalore, India. DNS, or 3,5-dinitrosalicylic acid ($C_2H_4N_2O_7$) (Cat. No: GRM1582), potassium sodium tartrate tetrahydrate ($C_4H_4KNaO_6.4H_2O$) (Cat. No: GRM1582), and sodium chloride (NaCl) (Cat. No: MB023), tris-hydrochloride ($C_4H_{11}NO_3$.HCL) (Cat. No: GRM613), trichloroacetic acid (TCA), ($C_2HCL_3O_2$) (Cat. No: GRM7570), Folin and Ciocalteu's Phenol Reagent (Cat. No: RM10822), sodium carbonate, anhydrous (GRM851), L-tyrosine (RM069), calcium chloride ($CaCl_2$) (MB034), ammonium carbonate (NH_4), and CO_3 (Cat. No: GRM1009) were purchased from HiMedia Laboratories, India. Sodium acetate, trihydrate ($C_2H_3NaO_2.3H_2O$) (Cat. No: 20235), SD Fine chemical, soluble starch $(C_6H_{10}O_5)_n$ (Cat. No: 14418), potassium chloride (KCL) (Cat. No: 50016), potassium dihydrogen orthophosphate (KH_2PO_4) (Cat. No: 54358), sodium bicarbonate ($NaHCO_3$) (Cat. No: 56398), and magnesium chloride hexahydrate $MgCl_2$ $(H_2O)_6$ (Cat. No: 54269) were purchased from Sisco Research Laboratories Pvt. Ltd. (SRL), Mumbai, India. Calcium acetate $(CH_2COO)_2$ Ca.x H_2O (Cat. No: H17) was purchased from Finar Limited, Gujarat, India.

2.2. Preparation of Stock Solution. The PS MPs and NPs were prepared as a stock solution (2 mg/mL) by suspending them in a phosphate-based buffer and a HCl (10 mM) depression medium. The PS particles were then dispersed using a sonicator for 30 min at room temperature. The brief experimental interaction system and concentrations used are shown in Table S1.

2.3. Interaction of PS-MNPs with Digestive Enzymes Using Multi Spectroscopic Analysis. MPs pose a significant threat to the environment and ecosystems as they can migrate into human health systems. Previous research articles have evaluated the quantity of MPs that humans might consume, providing a foundation for further studies. The risks to human health underscore the necessity of implementing preventive measures. According to the data from Senathirajah et al., 2021 humans may be ingesting an average of 0.1 to 5 g per week worldwide.[24,25]

Based on this information, the experiments for the current study were designed accordingly. The experimental system was performed using glass test tubes (5 mL). A control group (only digestive enzyme) and five different treatment groups (digestive enzymes) with varying concentrations of PS-MNPs (143, 173, 238, 357, and 714 μg/mL) were used. This setup aimed to assess the daily frequency of MPs intakes.

2.3.1. Fluorescence Spectrometry. Fluorescence spectroscopy was employed to study an in vitro simulated digestive fluid system model followed by previous articles.[25,26] This simulated digestive system comprises three segments: simulated salivary fluid (SSF), simulated gastric fluid (SGF), and simulated intestinal fluid (SIF). Based on the reports by refs 27 and 28, all simulated fluids were prepared accordingly and the compositions of the samples are represented in Table S2. The interacted mixture of plastics with different concentrations of digestive enzymes incubated at 37 °C was used to analyze the fluorescence emission spectrum.[23,29,30] This study was conducted based on the previous reports, and the concentration of PS-MNPs were fixed accordingly. They were used to interact with the simulated digestive fluid system SSF α-amylase (75 Units/mL) for 5 min, SGF pepsin (2000 Units/mL) for 2 h, and SIF pancreatin (100 Units/mL) for 2 h. Post the interaction process, all the incubated samples were analyzed using a fluorescence spectrophotometer (Model no. FP-8300, Serial No: C043561450) with an SCE-846 accessory and a Xe lamp light source, JASCO, Japan.

https://doi.org/10.1021/acsomega.4c07974
ACS Omega 2025, 10, 10866−10877

The enzyme excitation wavelengths (λex) were set as follows: salivary α-amylase at 276 nm, pepsin at 275 nm, and pancreatin at 258 nm. The measuring wavenumber range varies according to each enzyme up to 500 nm. The following parameters were fixed for all three enzymes: a response of 1 s, low sensitivity, a data interval of 1 nm, a scan speed of 500 nm/min, and bandwidths (λex) and (λem) of 5 nm. All of the experiments were conducted in triplicate and analyzed at room temperature. The Stern Volmer equation (eq 1)[31] was used to examine the type of quenching mechanism exhibited by the interaction of digestive enzymes with PS-MNPs. In the equation, F_o is the absence of PS-MNPs, F is the presence of PS-MNPs, K_{SV} is the Stern−Volmer quenching constant, K_q is the quenching constant, $\tau_0 = 10^{-8}$ s^{-1} (biomolecule average fluorophore lifetime), and [Q] is the cConcentration of PS-MNPs quenchers (μg/mL).[25,29,32]

$$\frac{F''}{F} = 1 + K_q\tau_o[Q] = 1 + K_{SV}[Q] \quad (1)$$

The synchronous fluorescence spectrometry (SFS) technique was used to the characterize the interactions of fluorescent amino acid residues such as tryptophan (Trp), tyrosine (Tyr), and phenylalanine (Phe) with quenchers in the microenvironment.[33] The synchronous spectrum was measured with two delta wavenumbers ($\Delta\lambda$) at 15 and 60 nm. The enzymes with the quencher aggregate and complex formation were analyzed using resonance light scattering (RLS) spectral measurement in the range of 200−800 nm. Similar parameters to those followed for the emission spectra were used for the synchronous and RLS study, except for the sensitivity parameter.

2.3.2. Fourier Transform Infrared Spectrometry. FT-IR spectrometric analysis was performed based on the previous experiments, where PS significantly reduced the fluorescence intensity of the enzymes. The concentration of enzymes used was similar to a previous experiment (Section 3.1) and the maximum concentration of PS (714 μg/mL) was used. The interaction sample mixtures were incubated at room temperature. All the samples were lyophilized and examined using a JASCO type A spectrometer (Model no.: FT/IR-6800), Japan (specification: 4 cm^{-1} precision, spectrum range 4000−400 cm^{-1}). The baseline correction data were transformed into absorbance spectra using Origin Pro 2022 software, and a deconvolution plot of absorption bands in the range of 1600−1700 cm^{-1} was created.[23,34,35]

2.3.3. Circular dichroism Spectrometry. Circular dichroism (CD) spectrometry analysis was done based on the results of fluorescence spectroscopy investigations (Section 3.1) from the study. The fluorescence studies of NPs resulted in a drastic decrease in the enzyme fluorescence intensity. The secondary structural alterations of digestive enzymes in the presence and absence of PS were investigated using a JASCO CD spectrometer (Model: J-815), Japan. The following parameters were used as stated: a quartz cell with a path length of 0.1 cm, two scans at a speed of 200 nm/min, and a spectral range of 180−250 nm. Enzymes similar to those in previous studies and the PS concentration (714 μg/mL) were consistently used. The interaction samples were mixed at room temperature and incubated.

2.4. Inhibition Activity Assay of Digestive Enzymes.

2.4.1. Salivary α-Amylase Inhibition Assay. The inhibition of human salivary α-amylase activity by PS-MNPs was assessed using previously cited methodologies.[23,36] In brief, sodium phosphate (20 mM) with a NaCl (6.7 mM) buffer solution was prepared. The DNS reagent was prepared using 3,5-dinitrosalicylic acid (96 mM) with potassium sodium tartrate tetrahydrate (5.3 mM). The interaction of the human salivary α-amylase (3 Units/mL) with different concentrations of the PS-MNPs mixture was prepared and incubated for 5 min at 37 °C (pH 6.9). Further, 400 μL of 1% starch solution was added to the mixture and incubated for 10 min at 37 °C. The reaction was then stopped by adding 400 μL of DNS solution and incubated in boiling water for 10 min. The hot interaction mixture was further kept at room temperature for cooling. Further, all the samples were filtered using a 0.1 μm filter, and the absorbance was measured at 540 nm (UV−Visible Bio Spectrometer basic, Eppendorf, Germany).

2.4.2. Pepsin Inhibition Assay. The inhibition assay of pepsin using PS-MNPs was carried out using previously reported methods.[27,37] In brief, the dilution solution of HCl (10 mM), 2% (w/v) of hemoglobin mixed in water at pH 2, and 4 mg/mL pepsin in 10 mM tris buffer and 150 mM NaCl at pH 6.5 was freshly made. The interactions were initiated by mixing different concentrations of PS-MNPs with 1000 Units/mL of pepsin and incubated for 2 h at 37 °C. After the interaction process, the enzyme activity assay was carried out with 100 μL of the interacted mixture solution and 500 μL of the hemoglobin substrate. Further, the solution was incubated for 10 min at 37 °C, and then, the reaction was stopped by adding 1 mL of 5% TCA solution. All the samples were filtered using a 0.1 μm filter, and the absorbance was measured at 280 nm.

2.4.3. Pancreatic Enzyme Inhibition Assay. The pancreatic enzyme interaction study was conducted using a standard concentration of the pancreatin enzyme (100 Units/mL) with different concentrations of PS-MNPs particles. Pancreatin is a combination of major digestive enzymes (α-amylase and protease). So, inhibition assays for both pancreatic α-amylase and protease have been studied.

2.4.3.1. Pancreatic α-Amylase Inhibition Assay. A similar protocol to that described in Section 2.4.1 was followed for the pancreatic α-amylase (pH 6.7−7.0) assay. Followed by the incubation period, 400 μL of 1% starch solution was added, and the mixtures were incubated for 10 min at 37 °C. The reaction was then stopped using DNS solution, followed by incubation in boiling water and sample filtration, consistent with the earlier assay. The absorbance measurements were taken at 540 nm.

2.4.3.2. Pancreatic Protease Inhibition Assay. The pancreatic protease inhibition assay was performed according to the previous studies cited by refs 27 and 38. In brief, a buffer solution was prepared using 50 mM potassium phosphate [dibasic, trihydrate (pH 7.5)] mixed with water. A substrate solution of 0.65% casein dissolved in the potassium phosphate buffer, 100 mM TCA solution, and 0.5 M Folin and Ciocalteu's phenol reagent (1:55) was used for the assay. The enzyme diluent solution was prepared using 500 mM sodium carbonate with 10 mM sodium acetate. The interaction of the pancreatin enzyme solution (100 Units/mL) with different concentrations of PS-MNPs was prepared and incubated at 37 °C for 2 h. After incubation, 5 mL of the substrate was added to the mixture and incubated at 37 °C for 5 min. The reaction was then stopped by adding 5 mL of TCA solution and incubated at 37 °C for 10 min. The reaction mixture was then centrifuged at 6000 rpm for 10 min. Subsequently, 2 mL of the supernatant was transferred to a fresh test tube and was mixed with 5 mL of sodium carbonate solution and 1 mL of Folin's reagent immediately. It was then incubated at 37 °C for 30 min. Finally, all the samples were

https://doi.org/10.1021/acsomega.4c07974
ACS Omega 2025, 10, 10866−10877

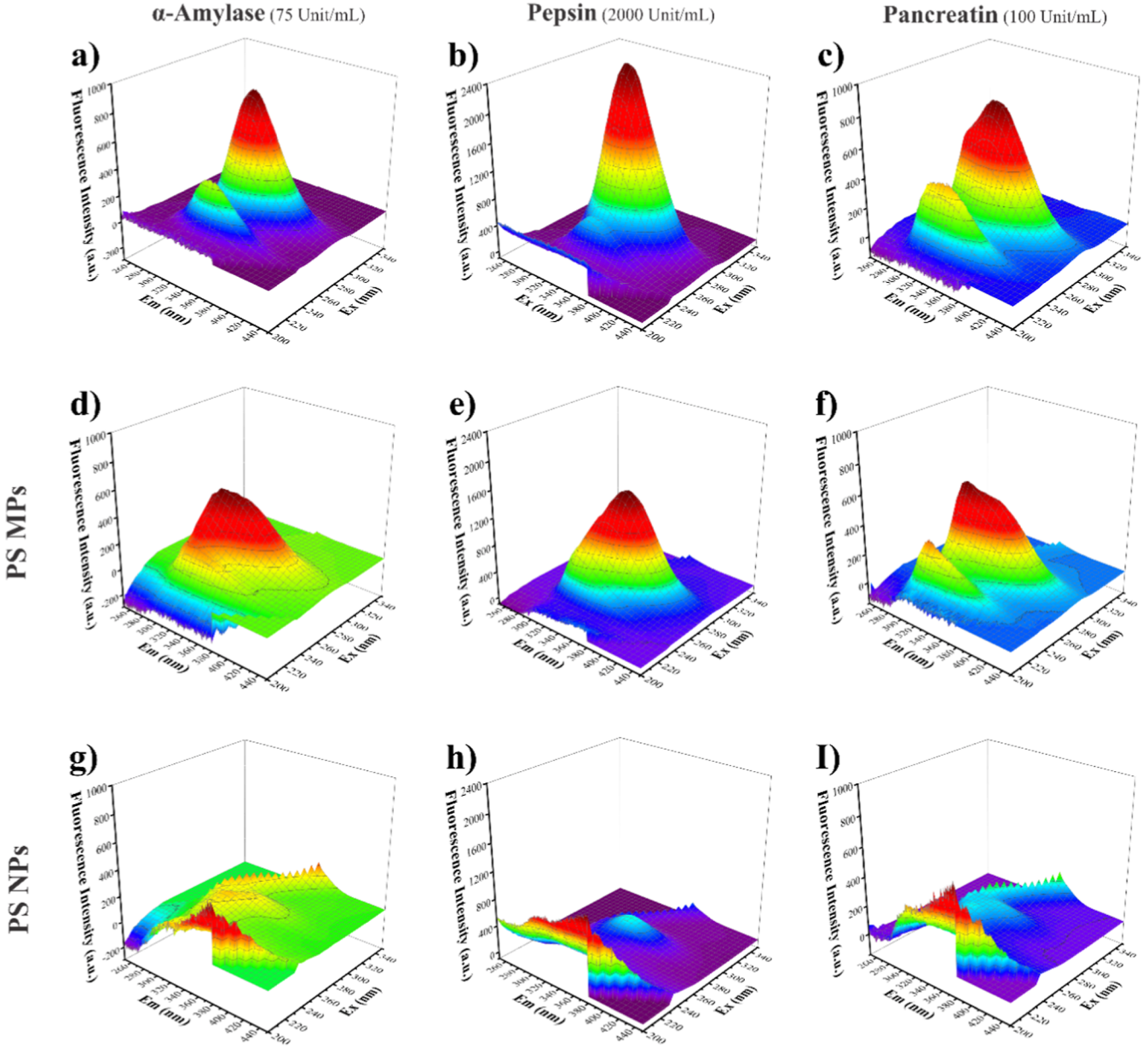

Figure 1. Digestive enzymes fluorescence emission (3D) spectrum maximum concentration of the quencher: (a−c) digestive enzyme controls; (d−f) PS MPs interacted with enzymes; and (g−i) PS NPs interacted with enzymes. Inside the figure: *X*-axis (emission wavenumber), *Y*-axis (fluorescence intensity), and *Z*- axis (excitation wavenumber).

filtered using a 0.1 μm filter, and the absorbance was measured at 660 nm.

The enzyme activity (%) was calculated using eq 2, the inhibition rate (%) was calculated using eq 3, and the half inhibitory concentration (IC_{50}) was calculated from the inhibition curve.[23,30]

$$\text{Enzyme activity (\%)} = (\text{Treated Abs} - \text{Control Abs}) \times 100 \quad (2)$$

$$\text{Inhibition rate (\%)} = \frac{\text{Control Abs} - \text{Treated Abs}}{\text{ControlAbs}} \times 100 \quad (3)$$

Here,

Control Abs—digestive enzymes absorbance;

Treated Abs—digestive enzyme interacted with PS MPs or PS NPs absorbance.

2.4.4. Determination of Inhibition Types. Based on the acquired results from the inhibition assays, the investigation of the inhibitory types of PS against digestive enzymes was carried according to the reported method followed by ref 30. The experiment was performed using standard concentrations of the digestive enzymes α-amylase (3 Units/mL), pepsin (1000 Units/mL), and pancreatin (100 Units/mL) interacted with the IC_{50} concentration of PS particles. After the incubation period, different concentrations of the substrate (starch: 12.4, 24.8, 37.1, 49.4, and 61.7 mM; hemoglobin: 4, 8, 12, 16, and 20 mg/mL; casein: 1.3, 2.6, 3.9, 5.2, and 6.5 mg/mL; and starch: 62, 124, 185.5, 247, and 308.5 mM) were added. Lineweaver−Burk plots generated by the Michaelis−Menten equation were used to

https://doi.org/10.1021/acsomega.4c07974
ACS Omega 2025, 10, 10866−10877

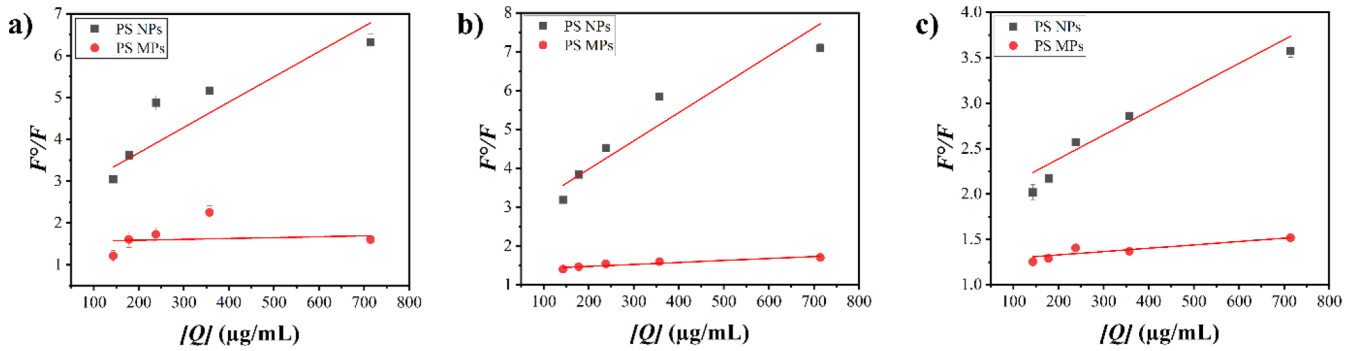

Figure 2. Mechanism of static quenching observed in both PS-MNPs as revealed by the Stern−Volmer plot, including (a) salivary α-amylase, (b) pepsin, and (c) pancreatin.

determine the maximal reaction velocity (V_{max}) and Michaelis constant (K_m).

2.4.5. Statistical Analysis. All the data sets analyzed during the study are expressed in the form of mean values (±) standard deviation. Data processing and analysis were performed using Microsoft Excel and Origin Pro 2022 software.

3. RESULTS AND DISCUSSION

3.1. Investigation of the Fluorescence Quenching Mechanism. The fluorescence quenching mechanism resulted from the interaction between PSMNP particles and digestive enzymes was investigated. The prepared PS-MNPs particles size was characterized (PS NPs: 100 nm and PS MPs: 37−50 μm in approximately) using FE-SEM analysis (Figure S1). These enzymes are composed of amino acids such as Trp and Tyr, which possess fluorescence property at specific wavelengths naturally.[32] Fluorescence spectroscopy is highly sensitive to the endogenous fluorophores present in the protein microenvironment.[39] The digestive enzymes pepsin (275 nm), pancreatin (258 nm), and α-amylase (276 nm) have different excitation wavelengths (λex). The results of the emission spectrum showed that the fluorescence quantum yield of the digestive enzyme decreased due to the increase in concentration of PS-MNPs. The resulted emission spectra caused due to the impacts of PS-MNPs is shown in Figure S1. Enzyme fluorescence intensity can be reduced by a number of mechanisms such as excited state reactions, energy transfer, complex formation, or collisional quenching.[40] In this sense, the main mode of quenching occurs when a PS-MNPs quencher molecule interacts with a fluorophore. The digestive enzymes used in the study show blue-shifting of the peak in quenchers. Subsequently, the static quenching method produces a ground-state complex, whereas dynamic quenching methods produce excited-state collision interactions.[41] Additionally, the maximum quencher concentration observations on the 3D spectrum are depicted in Figure 1. Figure 1 demonstrates that PS-NPs reduce the fluorescence intensity of enzymes more than PS MPs. Further, Stern−Volmer eq 1 was used to determine the fluorescence quenching mechanism.[34] The Stern−Volmer plot gives clarity on the interaction of PS-MNPs with digestive enzymes quenching fluorescence, as shown in (Figure 2 and Table 1). Stern−Volmer results (Table S3) display the K_q value. This is shown by the fact that the PS-MNPs (both) quenching rate constant is higher than the previously reported scattering collision quenching constant ($\sim 10^{10}$ $M^{-1}\cdot s^{-1}$),[42] which reveals the static quenching mechanism. Previous studies have found a similar mechanism for PS NPs interact with various biomolecules such as HSA,[43] α-amylase,[36] human salivary α-amylase,[23] and human hemoglobin.[44] These findings indicate that PS NPs impact the quantum yield of the fluorophore in digestive enzyme proteins by forming a nonfluorescent ground-state complex.

Table 1. Results of Static Quenching Mechanisms Determined by the Stern Volmer Plot

	PS MPs	PS NPs
	K_q ($\sim\times 10^{17}$ $M^{-1}\cdot s^{-1}$)	K_q ($\sim\times 10^{18}$ $M^{-1}\cdot s^{-1}$)
salivary α-amylase	2.711	3.638
pepsin	3.371	4.615
pancreatin	2.913	1.855

SFS was used to assess the structural alteration and peak shifting around Tyr and Trp residues in digestive enzymes.[32] As the PS MPs' concentration increases, a blue shift was observed at ($\Delta\lambda$) 15 and 60 nm for all the mixtures except pepsin and pancreatin at ($\Delta\lambda$) 15 nm, while increasing the PS NPs' concentration at ($\Delta\lambda$) 15 and 60 nm, all the results revealed a red shift, respectively, as shown in Table S4. The results indicate that PS NPs primarily alter Tyr and Trp amino acid residues, causing a red shift. This shift suggests changes in the digestive enzymes environment that lead to denaturation or loss of function more significantly than that by PS MPs. The peak shifting suggests decreased polarity and hydrophobicity around the fluorophore molecules.[23,32]

The states of aggregation and complex formation of PS-MNPs with digestive enzymes were determined by using an RLS spectrum. As the concentration of PS-MNPs increases, the intensity of the RLS spectrum peaks gradually increases, as shown in Figures S2−S4. The obtained results are due to the particle aggregation and complex formation during the interaction between digestive enzymes and PS-MNPs.[36] The results coincides with the our previous reports in refs 23 and 36

From the comparative analysis of fluorescence spectroscopy studies with MNPs, it was identified that PS MPs interaction with salivary α-amylase and pancreatin did not show quenching at the maximum concentration (Figure S2); instead, PS MPs induced the fluorescence intensity. In contrast, with increasing concentrations of PS NPs, there was a significant decrease in fluorophore quantum yield and fluorescence intensity, along with an effect on Trp and Tyr amino acids with a red shift. Based on the obtained data, further investigations were done to identify the interaction of PS NPs with the digestive enzyme and its secondary structural changes in detail using FT-IR and CD spectrometry analysis.

3.2. FT-IR Analysis. The fluorescence spectrum study revealed that PS NPs significantly reduce the enzyme

https://doi.org/10.1021/acsomega.4c07974
ACS Omega 2025, 10, 10866−10877

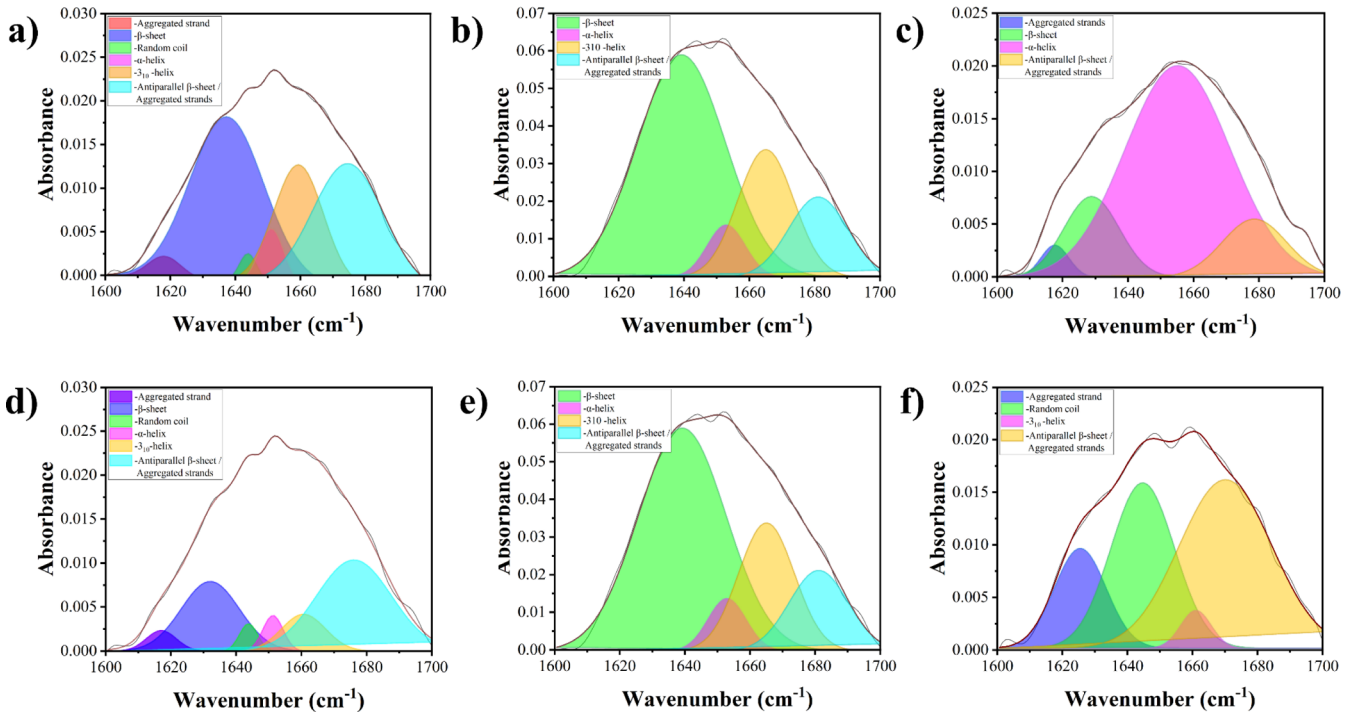

Figure 3. FT-IR absorbance spectrum results illustrating the effect of PS NPs on the secondary structure amide band I of the digestive enzyme, including (a−c) without PS NPs and (d−f) with PS NPs (714 μg/mL), in the following order: (a) salivary α-amylase, (b) pepsin, and (c) pancreatin.

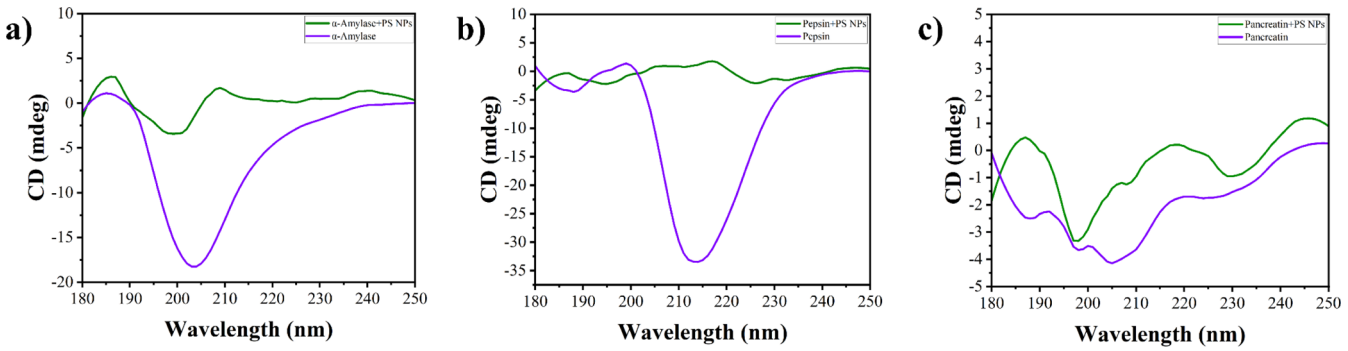

Figure 4. CD spectrometry results showing the effect of the PS NPs secondary structure of digestive enzymes. Includes (a−c) without PS NPs and (d−f) with PS NPs (714 μg/mL), in the following order: (a) salivary α-amylase, (b) pepsin, and (c) pancreatin.

fluorophore characteristics. Additionally, the maximum concentration of PS NPs with digestive enzymes was examined using an FT-IR spectrometer to analyze the changes in protein secondary structures and specific amide band peaks, which correspond to the vibrations of different peptide moieties. The frequency of vibrations in the amide band is closely associated with the secondary structure of proteins. The amide I band, which usually appears between 1600 and 1700 cm^{-1}, indicates the secondary structure by reflecting the direction of digestive enzymes.[23,45] C═O stretching vibrations make up the majority of its components. The primary source of amide I is the stretching vibrations of hydrogen bonds in acid amides and amino acid residues.[23,46] The overlapping curve fit to the enzyme absorbance spectrum was used for identifying the hidden peaks. This was obtained by converting the acquired data into an absorbance spectrum using a peak-analyzer deconvolution plot.[35] We can identify the percentage (%) of specific secondary structure components such as the α-helix, β-sheet, 3^{10}-helix, and random coil properties.[34,45] The secondary structure component content (%) was compared with that of the literature references.

The FT-IR technique was used to interpret the results of the interaction between PS NPs and digestive enzymes in both ways (with and without PS NPs). The secondary structure content (%) of the amide I band and its characteristics are shown in Figure 3 and Tables S5−S7. A deconvolution plot was applied to summarize the obtained data. When the enzymes interacted with PS NPs, the secondary structure content (%) of α-amylase was reduced as detailed below. This included the reduction of α-helix (4.5 to 2.4%), 3$_{10}$-helix (20.5 to 5.4%), random coils (1.7 to 1.6%), and β-sheets/aggregated strands (29.8 to 22.8%); pepsin: β-sheets (58.5 to 21.5%), α-helix (6 to 0%), and antiparallel β-sheet/aggregated strands (14.1 to 9.1%); and pancreatin: β-sheets (14.2 to 0%), α-helix (70.3 to 0%), and antiparallel β-sheet/aggregated strands (11.8 to 0%). An increase in secondary structure content (%) was observed in pepsin of 3$_{10}$-helix (21.3 to 63.3%) and in pancreatin of aggregated strands (2.8 to 15.9%).

https://doi.org/10.1021/acsomega.4c07974
ACS Omega 2025, 10, 10866−10877

Table 2. CD Spectrometry Results Illustrating the Effect of PS NPs on the Changes in Secondary Structure Protein Content (%) of Digestive Enzymes

secondary structure	secondary structure protein content (%)					
	Salivary α-amylase	Salivary α-amylase + PS NPs	Pepsin	Pepsin + PS NPs	Pancreatin	Pancreatin + PS NPs
α-helix	0	0	13.5	0	7.6	0
β-sheet	59.8	0	45	0	33.1	0
turn	0	0	14.2	41.4	15.5	15.8
random	40.2	100	27.2	58.6	43.9	84.2

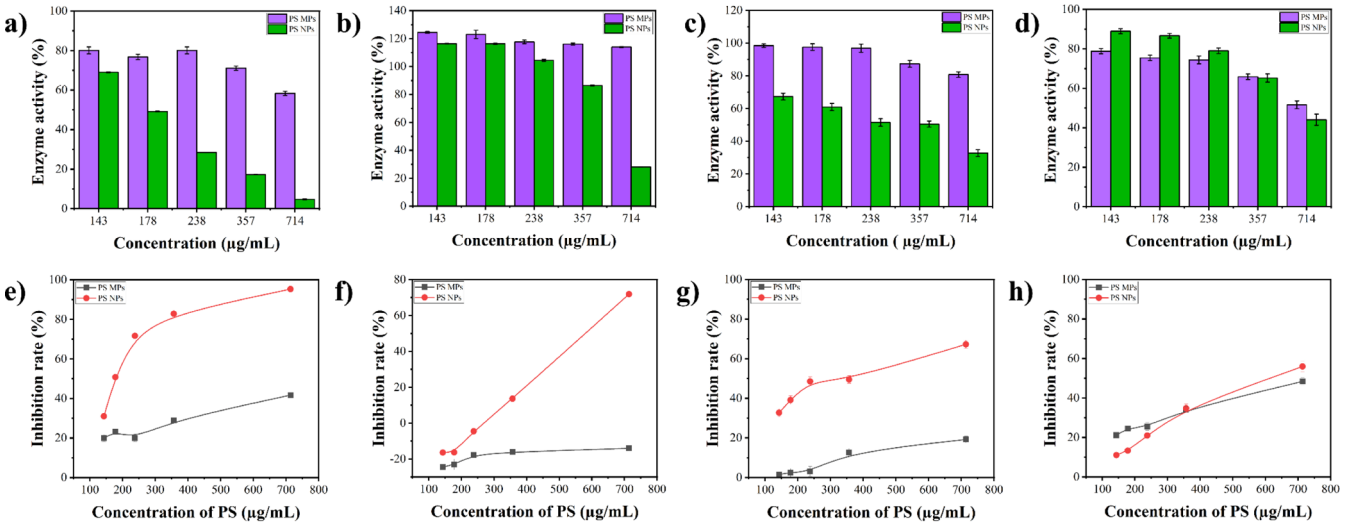

Figure 5. Interaction between PS-MNPs and digestive enzymes, showing (a–d) enzyme activity (%) and (e–h) inhibition rate (%). The order is as follows: salivary α-amylase, pepsin, pancreatic protease, and pancreatic α-amylase.

During the interaction of PS NPs with digestive enzymes, the amide I band results show the changes in secondary structural protein content (%) fluctuation. It was observed that the changes in frequency significantly decrease protein contents (%) of the β-sheets, α-helix, and antiparallel β-sheet/aggregated in all the enzymes studied. These changes can lead to destabilization of the β-sheet, affecting the overall stability and function of the protein, disruption of the hydrogen bonding network that stabilizes α-helices, and potential protein aggregation.[47,48] Besides, a decrease in the major secondary structure protein content (%) may affect the function and activity of digestive enzymes also.

3.3. CD Spectrometry. The CD technique is an excellent method for rapid assessment of protein secondary structure, folding, and binding characteristics as different structural components produce distinct CD spectra. The major protein secondary structures are the α-helix and β-sheet. The α-helix structure is characterized by a negative band at 190 nm and positive bands at 208 and 222 nm. In contrast, β-sheets exhibit more variable spectra with a positive band around 198 nm and a negative band between 214–218 nm depending on the specific type of the structure.[49] The interaction between PS NPs and digestive enzymes was examined by using CD spectra in the presence and absence of PS NPs. The results and secondary structural protein content (%) are illustrated in (Figure 4) and (Tables 2). Upon interaction with PS NPs, there was a notable decrease in the major secondary structures, specifically α-helix and β-sheet. For α-amylase, the β-sheet content decreased from 59.8 to 0%. In the case of pepsin, the α-helix content dropped from 13.5 to 0% and the β-sheet content dropped from 45 to 0%. Similarly, for pancreatin, the α-helix content decreased from 7.6 to 0% and the β-sheet content decreased from 33.1 to 0%. Consequently, there was an increase in β-turn in pepsin (14.2 to 41.4%) and pancreatin (15.5 to 15.9%). The results reveal that PS NPs have an impact on digestive enzymes. A decrease in α-helix and β-sheet in the secondary structure indicated a strong structural alteration of the digestive enzyme's native structure, which sequentially affects the enzyme activity. These results coincide with the FT-IR data obtained from the current study.

3.4. Inhibition Activity Assay of the Digestive Enzyme. *3.4.1. Salivary α-Amylase Inhibition Assay.* The inhibitory effects of PS-MNPs on α-amylase were examined. The α-amylase interacted with various concentrations of PS-MNPs, and DNS methods were used to measure the activity of the α-amylase, respectively, as shown in Figure 5a,e. While increasing the PS-MNPs concentration, the α-amylase activity gets inhibited, leading to the deceleration of the starch hydrolysis process. The maximum inhibition concentration result shows the inhibition percentage of salivary α-amylase for PS MPs to be 41.67% and for PS NPs to be 95.28%. The inhibition assay showed that the PS NPs strongly inhibit the functions of salivary α-amylase activity, with an observed IC_{50} value of 180 μg/mL (Figure S5). Further, these results were analogous to our previous report on diastase α-amylase with PS NPs and human salivary α-amylase with PS NPs.[23,36] This reveals that an increase in PSNPs eventually decreases the salivary α-amylase activity. The salivary α-amylase enzyme inhibition has significant effects on the human digestive system, encompassing gastrointestinal issues, metabolic disorders,[42] and type II diabetes[43] as well.

3.4.2. Pepsin Inhibition Assay. The interaction between pepsin and PS-MNPs was investigated using an inhibition assay, as shown in Figure 5b,f. The findings reveal that increasing the

https://doi.org/10.1021/acsomega.4c07974
ACS Omega 2025, 10, 10866–10877

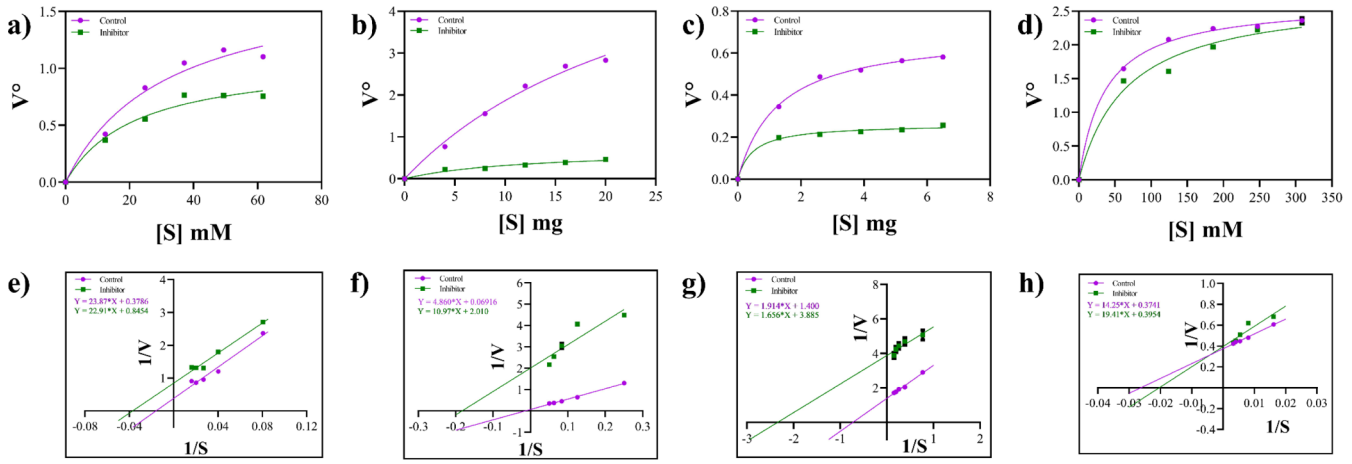

Figure 6. IC_{50} concentration of PS NPs used for determining types of inhibition in digestive enzymes, including (a−d) velocity reaction (%) and (e−h) Lineweaver−Burk double reciprocal plots.

concentration of PS-MNPs inhibits the function of the pepsin enzyme, when assessed with the hemoglobin substrate. At the higher concentration of PS-MNPs, pepsin is inhibited, indicating the lowering of hemoglobin hydrolysis. The maximum inhibition percentages of pepsin were decreased to 2.6% for PS MPs and 64.2% for PS NPs. The inhibition assay clearly demonstrated that PS NPs strongly inhibit pepsin activity with an IC_{50} value of 580 μg/mL, as shown in Figure S5. Pepsin enzyme inhibition can negatively impact the stomach, causing gastroesophageal reflux disease.[50]

3.4.3. Pancreatic Enzyme Inhibition Assay. 3.4.3.1. Pancreatic α-Amylase Inhibition Assay. A similar procedure to that described in Section 3.1 was followed to measure the activity of pancreatic α-amylase. The results are shown in Figure 5d,h. The maximum inhibition percentages for pancreatic α-amylase were observed to be 48.38% with PS MPs and 55.93% with PS NPs. Notably, the inhibition assay demonstrated that PS NPs strongly suppress the function of pancreatic α-amylase, with an observed IC_{50} value of 314 μg/mL (see Figure S5). This inhibition of pancreatic α-amylase activity has significant health implications for the human digestive system.

3.4.3.2. Pancreatic Protease Inhibition Assay. The interaction between pancreatic protease and PS-MNPs was investigated, and the results are shown in Figure 5c. The findings reveal that increasing the concentration of PS-MNPs inhibit the activity of the protease enzyme, thus reducing the hydrolysis of casein protein. The maximum inhibition percentages for pancreatic protease were observed to be 19.2% with PS MPs and 67.3% with PS NPs, as shown in Figure 5g. PS NPs strongly inhibit protease activity with an IC_{50} value of 314 μg/mL, as shown in Figure S5. Inhibition of pancreatic protease may induce the human gastrointestinal diseases, inflammatory bowel diseases, and colorectal cancer.[51]

From the enzyme activity (%) and inhibition rate (%) data, it was identified that PS NPs highly inhibit digestive enzyme activity when compared to PS MPs. From the obtained PS NPs (IC_{50}) concentration, the types of inhibition mechanisms were further determined.

3.4.4. Determination of Digestive Enzyme Inhibition Types. Followed by these results, steady-state enzyme kinetics was used to identify the variety of mechanisms through which these reversible inhibitors function.[52] The type of inhibition for the digestive enzymes assessed in the study was determined with PS NPs (IC_{50}) concentration. The velocity of an enzyme reaction using various substrate concentrations with and without inhibitors was studied similar to the reports of ref 30. The data are displayed using Lineweaver−Burk double reciprocal plots, as shown in Figure 6, indicating the inhibition of the digestive enzyme. This study reveals that both the V_{max} and K_m values decreased as shown in Table 3. The results indicating

Table 3. Types of Inhibition Determined by IC_{50} Concentration of PS NPs with Digestive Enzymes

enzymes	K_m (μg/mL)	V_{max} (μg/mL·min)	inhibition types
salivary α-amylase (without the inhibitor)	31.41	1.81	
salivary α-amylase (PS NPs inhibitor)	21.92	1.09	uncompetitive
pepsin (without the inhibitor)	27.65	7.03	
pepsin (PS NPs inhibitor)	11.94	0.70	uncompetitive
pancreatic protease (without the inhibitor)	1.27	0.70	
pancreatic protease (PS NPs inhibitor)	0.48	0.26	uncompetitive
pancreatic α-amylase (without the inhibitor)	36.39	2.64	
pancreatic α-amylase (PS NPs inhibitor)	66.15	2.74	mixed inhibition

salivary α-amylase, pepsin, and pancreatic protease reveal uncompetitive inhibition, whereas pancreatic α-amylase shows a mixed type of inhibition.[53] The uncompetitive inhibitor binds to the ES complex alone, not the free enzyme.[53] In the mixed type of inhibition, the inhibitor can bind to both the free enzyme (E) and the ES complex.[54] Aside from this feature, the ES−inhibitor (ESI) complex does not produce a product due to the enzyme's conformational changes.[55] Accordingly, the types of inhibition mechanism followed are shown in Figure 7. This study gives an overview of the enzyme activity and inhibition types. The study reveals that PS NPs highly inhibit digestive enzyme activity. The enzyme inhibitory assay demonstrates that the greater the concentration of PS NPs, the slower the enzyme reaction rate. This process gives a clarity on the reversible enzyme inhibition mechanism, which involves an inhibitor molecule binding reversibly to enzymes.[52] Significantly, previous results shown in Table 4 highlight the interaction between MNPs and biomolecules, including its implications.

https://doi.org/10.1021/acsomega.4c07974
ACS Omega 2025, 10, 10866−10877

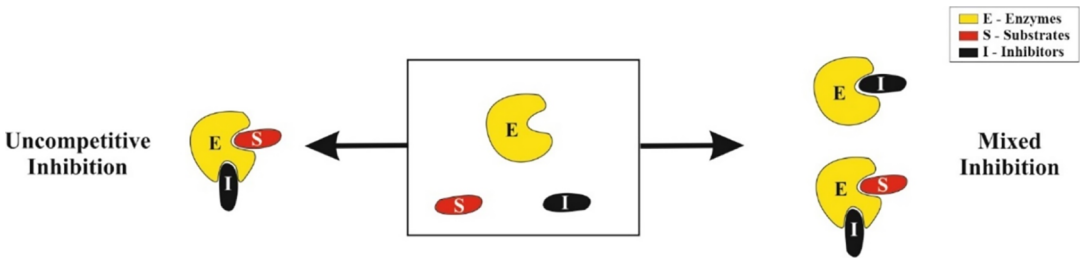

Figure 7. Schematic representation of inhibition types of mechanisms, where (E) stands for the enzyme (digestive enzymes), (S) stands for the substrate (starch, hemoglobin, and casein), and (I) stands for the inhibitor (PS NPs).

Table 4. MNPs Interactions with Biomolecules and Their Implications

S. No	Interactions	Plastics concentrations	Outcomes	References
1	PS NPs with human salivary α-amylase	PS NPs (20, 40, 60, 80, and 100 μg/mL)	•PS NPs competitively inhibit α-AHS enzyme activity, causing structural changes •PS NPs interact with α-AHS, leading to conformational alterations and functional impact	23
2	effects of oolong tea polyphenols, EGCG, and EGCG3 with pancreatic α-amylase	effects of oolong tea polyphenols, EGCG, and EGCG3 (0.1 mg/mL)	•EGCG had the highest inhibitory potency against a-amylase •EGCG3″Me showed a weaker inhibitory effect due to structural differences •oolong tea polyphenols have antiobesity and hyperlipidemic effects	30
3	PVC with HSA	PVC (0−70 μg/mL)	•PVC MPs interact with HSA through static quenching, driven by electrostatic forces •PVC MPs induce microenvironment changes in HSA, decreasing the α-helix structure •the study provides insights into PVC−HSA interaction and potential biological toxicity	29
4	PSNPs with HSA	PSNPs (0−100 μg/mL)	•PSNPs bind to HSA, altering its structure and reducing esterase activity •PSNPs interact with aromatic amino acids in subdomain IIA of HSA •structural changes in HSA by PSNPs may affect its physiological function	43
5	PSNPs, PS-COOH, and PS-NH_2 with HSA	PSNPs, PS-COOH, and PS-NH_2 (0, 50, and 100 μg/mL)	•PS-NH2 affects the protein conformation; smaller NPs impact the structure more •PSNPs inhibit HSA esterase activity; PS-NH2 shows the greatest reduction •smaller NPs increase protein reactivity; larger NPs weaken protein interaction	57
6	PSNPs, PS-COOH, and PS-NH_2 with hemoglobin	PSNPs, PS-COOH, and PS-NH_2 (0−50 μg/mL)	•PS NPs interact with Hb, altering the structure and function •PS-NH_2 has the most significant effect on Hb conformation •PS-COOH binds via hydrogen bonding, PS and PS-NH_2 via hydrophobic force •the minimal absorbance peak shift indicates enhanced hydrophobicity by PS-NH_2 •NPs penetrate protein surfaces, causing structural changes in Hb	44
7	PSNPs with diastase α-amylase	PSNPs (20, 40, 60, 80, and 100 μg/mL)	•investigates PSNPs interaction with plant α-amylase and its effects •examines structural changes in α-amylase due to PSNPs interaction	36
8	PS MPs with lipid	PS MPs (100, 200, 300, and 400 mg/L)	•MPs inhibit lipid digestion in the gastrointestinal system •PS MPs reduce lipid digestion by forming large lipid−MPs heteroaggregates •PS MPs adsorb lipase, changing its structure and reducing activity •interaction plays a crucial role in lipid digestion reduction	22

Digestive enzymes facilitate the breakdown of complex molecules, such as starch and proteins, through hydrolysis. This plays a crucial role in the human digestive process and metabolism, significantly implicating the overall health.[56] The interaction of MNP pollutants with digestive enzymes such as α-

https://doi.org/10.1021/acsomega.4c07974
ACS Omega 2025, 10, 10866−10877

amylase, pepsin, and pancreatin, as well as their toxicological influence, should be investigated when consumed by humans.

4. CONCLUSIONS

In this human model microenvironmental in vitro study, we delved into the intricate interaction between PS-MNPs and digestive enzymes. Analytical techniques such as fluorescence spectroscopy, FT-IR spectroscopy, CD spectrometry, enzyme inhibition assays, and inhibition-type determination were explored to unravel the effects of PS-MNPs on enzyme behavior. The PS NPs exhibit a remarkable affinity for enzymes, leading to structural modifications. The fluorescence emission spectra revealed a significant reduction in the enzyme fluorescence quantum yield. The Stern−Volmer equation was used to identify the static quenching mechanism across the digestive enzymes assessed in the study. Notably, PS NPs predominantly affect the Tyr and Trp residues. The RLS spectra confirmed the formation of enzyme−PS NP complexes followed by aggregation. FTIR and CD spectrometry results revealed a decrease in the (α-helix and β-sheet) major secondary structure of protein, which can lead to destabilization of the enzymes. These conformational changes may influence enzyme functionality also. Inhibition of enzyme activity: PS NPs inhibit enzyme activity more than PS MPs. The IC_{50} values for PS NPs indicated uncompetitive and mixed and reversible inhibition of digestive enzymes. Interestingly, increased exposure to NPs could potentially decrease metabolic activity due to structural alterations in digestive enzymes. To conclude, the current study unravels the implications of PS NPs (100 nm) on human health by slowing down the digestive process (enzymatic inhibition). Understanding these effects are crucial for assessing the impact of environmental pollutants such as PS NPs on digestive enzyme function and overall health.

The current study contributes to the understanding of the impact of environmental pollutants on human health. By highlighting the health risks of PS-MNPs, this research supports the development of strategies to mitigate MP pollution and protect public health.

ASSOCIATED CONTENT

Supporting Information

The Supporting Information is available free of charge at https://pubs.acs.org/doi/10.1021/acsomega.4c07974.

PS MPs (PS MPs) (37−50 μm) and PS NPs (100 nm); digestive enzymes fluorescence emission spectrum: PS MPs and PS NPs interactions; synchronous spectrum and RLS of salivary α-amylase with PS MPs and PS NPs; synchronous spectrum and RLS of pepsin with PS MPs and PS NPs; synchronous spectrum and RLS of pancreatin with PS MPs and PS NPs; IC_{50} concentration of PS NPs determined by inhibition (%); summary of experiments, enzymes, and PS-MNPs concentrations; composition of simulated fluid solutions; data of static quenching mechanism values (K_{SV} and K_q); synchronous fluorescence spectrum peak shifting during enzyme interaction with PS MPs and PS NPs; FT-IR absorbance spectrum results for salivary α-amylase with PS NPs; FT-IR absorbance spectrum results for pepsin with PS NPs; and FT-IR absorbance spectrum results for pancreatin with PS NPs (PDF)

AUTHOR INFORMATION

Corresponding Author

Natarajan Chandrasekaran − *Centre for Nanobiotechnology, Vellore Institute of Technology (VIT), Vellore, Tamil Nadu 632014, India*; orcid.org/0000-0002-0586-134X; Email: nchandrasekaran@vit.ac.in, /nchandra40@hotmail.com

Author

Ananthaselvam Azhagesan − *Centre for Nanobiotechnology, Vellore Institute of Technology (VIT), Vellore, Tamil Nadu 632014, India*

Complete contact information is available at: https://pubs.acs.org/10.1021/acsomega.4c07974

Notes

The authors declare no competing financial interest.

ACKNOWLEDGMENTS

We immensely acknowledge the Indian Council of Medical Research (ICMR), New Delhi, Government of India (ICMR-SRF) [File no. 3/1/2(14)/Evn/2021-NCD-II] for the financial support and Vellore Institute of Technology (VIT) for providing the lab facilities to carry out the research work.

ABBREVIATIONS

PS	polystyrene
PS-MNPs	polystyrene micro- and nanoplastics
PS NPs	polystyrene nanoplastics
PS MPs	polystyrene microplastics
Tyr	tyrosine
Trp	tryptophan
SFS	synchronous fluorescence spectrometry
RLS	resonance light scattering
FT-IR	Fourier transform infrared
IC_{50}	half inhibitory concentration
CD	circular dichroism

REFERENCES

(1) Kibria, M. G.; Masuk, N. I.; Safayet, R.; Nguyen, H. Q.; Mourshed, M. Plastic Waste: Challenges and Opportunities to Mitigate Pollution and Effective Management. *Int. J. Environ. Res.* **2023**, *17*, 20.

(2) Pan, D.; Su, F.; Liu, C.; Guo, Z. Research progress for plastic waste management and manufacture of value-added products. *Adv. Compos. Hybrid Mater.* **2020**, *3*, 443−461.

(3) Gopinath, P. M.; Saranya, V.; Vijayakumar, S.; Mythili Meera, M.; Ruprekha, S.; Kunal, R.; Pranay, A.; Thomas, J.; Mukherjee, A.; Chandrasekaran, N. Assessment on interactive prospectives of nanoplastics with plasma proteins and the toxicological impacts of virgin, coronated and environmentally released-nanoplastics. *Sci. Rep.* **2019**, *9*, 8860.

(4) Guerranti, C.; Martellini, T.; Perra, G.; Scopetani, C.; Cincinelli, A. Microplastics in cosmetics: Environmental issues and needs for global bans. *Environ. Toxicol. Pharmacol.* **2019**, *68*, 75−79.

(5) Derraik, J. G. B. The pollution of the marine environment by plastic debris: a review. *Mar. Pollut. Bull.* **2002**, *44*, 842−852.

(6) Picó, Y.; Barceló, D. Analysis of microplastics and nanoplastics: How green are the methodologies used? *Curr. Opin. Green Sustainable Chem.* **2021**, *31*, 100503.

(7) Acharya, S.; Rumi, S.; Hu, Y.; Abidi, N. Microfibers from synthetic textiles as a major source of microplastics in the environment: A review. *Text. Res. J.* **2021**, *91*, 2136−2156.

(8) Okunola, A. A.; Kehinde, I. O.; Oluwaseun, A.; Olufiropo, E. A. Public and Environmental Health Effects of Plastic Wastes Disposal: A Review. *J. Toxicol. Risk Assess.* **2019**, *5*, 1−13.

(9) Mofijur, M.; Ahmed, S. F.; Rahman, S. A.; Arafat Siddiki, S. Y.; Islam, A. S.; Shahabuddin, M.; Ong, H. C.; Mahlia, T.; Djavanroodi, F.; Show, P. L. Source, distribution and emerging threat of micro- and nanoplastics to marine organism and human health: Socio-economic impact and management strategies. *Environ. Res.* **2021**, *195*, 110857.
(10) Fadare, O. O.; Wan, B.; Guo, L. H.; Zhao, L. Microplastics from consumer plastic food containers: Are we consuming it? *Chemosphere* **2020**, *253*, 126787.
(11) Mercogliano, R.; Avio, C. G.; Regoli, F.; Anastasio, A.; Colavita, G.; Santonicola, S. Occurrence of microplastics in commercial seafood under the perspective of the human food chain. A review. *J. Agric. Food Chem.* **2020**, *68*, 5296−5301.
(12) Sun, A.; Wang, W.-X. Human Exposure to Microplastics and Its Associated Health Risks. *Environ. Health* **2023**, *1*, 139−149.
(13) Kutralam-Muniasamy, G.; Shruti, V. C.; Pérez-Guevara, F.; Roy, P. D. Microplastic diagnostics in humans: "The 3Ps" Progress, problems, and prospects. *Sci. Total Environ.* **2023**, *856*, 159164.
(14) Yin, K.; Wang, Y.; Zhao, H.; Wang, D.; Guo, M.; Mu, M.; et al. A comparative review of microplastics and nanoplastics: Toxicity hazards on digestive, reproductive and nervous system. *Sci. Total Environ.* **2021**, *774*, 145758.
(15) Yee, M. S. L.; Hii, L. W.; Looi, C. K.; Lim, W. M.; Wong, S. F.; Kok, Y. Y.; Tan, B. K.; Wong, C. Y.; Leong, C. O. Impact of microplastics and nanoplastics on human health. *Nanomaterials* **2021**, *11*, 496.
(16) Xiang, Y.; Jiang, L.; Zhou, Y.; Luo, Z.; Zhi, D.; Yang, J.; et al. Microplastics and environmental pollutants: Key interaction and toxicology in aquatic and soil environments. *J. Hazard. Mater.* **2022**, *422*, 126843.
(17) Wang, Q.; Huang, F.; Liang, K.; Niu, W.; Duan, X.; Jia, X.; et al. Polystyrene nanoplastics affect digestive function and growth in juvenile groupers. *Sci. Total Environ.* **2022**, *808*, 152098.
(18) Kim, L.; Cui, R.; Il Kwak, J.; An, Y. J. Trophic transfer of nanoplastics through a microalgae−crustacean−small yellow croaker food chain: Inhibition of digestive enzyme activity in fish. *J. Hazard. Mater.* **2022**, *440*, 129715.
(19) Peyrot des Gachons, C.; Breslin, P. A. S. Salivary Amylase: Digestion and Metabolic Syndrome. *Curr. Diabetes Rep.* **2016**, *16*, 102.
(20) Rio, A. D.; Keppler, J.; Boom, R.; Function, A. J.-F. Protein acidification and hydrolysis by pepsin ensure efficient trypsin-catalyzed hydrolysis. *PubsRscOrg.* **2021**, *12*, 4570 undefined.
(21) Pandol, S. J. Normal Pancreatic Function. *Pancreapedia* **2015**, 13.
(22) Tan, H.; Yue, T.; Xu, Y.; Zhao, J.; Xing, B. Microplastics Reduce Lipid Digestion in Simulated Human Gastrointestinal System. *Environ. Sci. Technol.* **2020**, *54*, 12285−12294.
(23) Azhagesan, A.; Rajendran, D.; Varghese, R. P.; George Priya Doss, C.; Chandrasekaran, N. Assessment of polystyrene nano plastics effect on human salivary α-amylase structural alteration: Insights from an in vitro and in silico study. *Int. J. Biol. Macromol.* **2024**, *257*, 128650.
(24) Senathirajah, K.; Attwood, S.; Bhagwat, G.; Carbery, M.; Wilson, S.; Palanisami, T. Estimation of the mass of microplastics ingested − A pivotal first step towards human health risk assessment. *J. Hazard. Mater.* **2021**, *404*, 124004.
(25) Tamargo, A.; Molinero, N.; Reinosa, J. J.; Alcolea-Rodriguez, V.; Portela, R.; Bañares, M. A.; et al. PET microplastics affect human gut microbiota communities during simulated gastrointestinal digestion, first evidence of plausible polymer biodegradation during human digestion. *Sci. Rep.* **2022**, *12*, 1−15.
(26) Chen, H.; Chen, H.; Nan, S.; Liu, H.; Chen, L.; Yu, L. Investigation of Microplastics in Digestion System: Effect on Surface Microstructures and Probiotics. *Bull. Environ. Contam. Toxicol.* **2022**, *109*, 882−892.
(27) Brodkorb, A.; Egger, L.; Alminger, M.; Alvito, P.; Assunção, R.; Ballance, S.; et al. INFOGEST static in vitro simulation of gastrointestinal food digestion. *Nat. Protoc.* **2019**, *14*, 991−1014.
(28) Minekus, M.; Alminger, M.; Alvito, P.; Ballance, S.; Bohn, T.; Bourlieu, C.; et al. A standardised static in vitro digestion method suitable for food-an international consensus. *Food Funct.* **2014**, *5*, 1113−1124.
(29) Ju, P.; Zhang, Y.; Zheng, Y.; Gao, F.; Jiang, F.; Li, J.; et al. Probing the toxic interactions between polyvinyl chloride microplastics and Human Serum Albumin by multispectroscopic techniques. *Sci. Total Environ.* **2020**, *734*, 139219.
(30) Fei, Q.; Gao, Y.; Zhang, X.; Sun, Y.; Hu, B.; Zhou, L.; et al. Effects of Oolong tea polyphenols, EGCG, and EGCG3″Me on pancreatic α-amylase activity in vitro. *J. Agric. Food Chem.* **2014**, *62*, 9507−9514.
(31) Soares, S.; Mateus, N.; De Freitas, V. Interaction of Different Polyphenols with Bovine Serum Albumin (BSA) and Human Salivary α-Amylase (HSA) by Fluorescence Quenching. *J. Agric. Food Chem.* **2007**, *55*, 6726−6735.
(32) Falese, B. A.; Kolawole, A. N.; Sarumi, O. A.; Kolawole, A. O. Probing the interaction of iminium form of sanguinarine with human salivary α-amylase by multi-spectroscopic techniques and molecular docking. *J. Mol. Liq.* **2021**, *334*, 116346.
(33) Sunuwar, S.; Manzanares, C. E. Excitation, emission, and synchronous fluorescence for astrochemical applications: Experiments and computer simulations of synchronous spectra of polycyclic aromatic hydrocarbons and their mixtures. *Icarus* **2021**, *370*, 114689.
(34) (a) Jackson, M. HM-C reviews in biochemistry. The use and misuse of FTIR spectroscopy in the determination of protein structure, **1995** undefined (b) Jackson, M.; Mantsch, H. H. The use and misuse of FTIR spectroscopy in the determination of protein structure. *Crit. Rev. Biochem. Mol. Biol.* **1995**, *30*, 95−120.
(35) Sadat, A.; Joye, I. J. Peak fitting applied to fourier transform infrared and raman spectroscopic analysis of proteins. *Appl. Sci.* **2020**, *10*, 5918.
(36) Azhagesan, A.; Chandrasekaran, N.; Mukherjee, A. Multi-spectroscopy analysis of polystyrene nanoplastic interaction with diastase α-amylase. *Ecotoxicol. Environ. Saf.* **2022**, *247*, 114226.
(37) Anson, M. L. The Estimation of Pepsin, Trypsin, Papain, and Cathepsin With Hemoglobin. *J. Gen. Physiol.* **1938**, *22*, 79−89.
(38) Lowry, O. H.; Rosebrough, N. J.; Farr, A. L.; Randall, R. J. Protein Measurement With The Folin Phenol Reagent. *J. Biol. Chem.* **1951**, *193*, 265−275.
(39) Lu, Q.; Chen, C.; Zhao, S.; Ge, F.; Liu, D. Investigation of the Interaction Between Gallic Acid and α-Amylase by Spectroscopy. *Int. J. Food Prop.* **2016**, *19*, 2481−2494.
(40) Mátyus, L.; Szöllosi, J.; Jenei, A. Steady-state fluorescence quenching applications for studying protein structure and dynamics. *J. Photochem. Photobiol., B* **2006**, *83*, 223−236.
(41) Lehrer, S. S. Solute perturbation of protein fluorescence. Quenching of the tryptophyl fluorescence of model compounds and of lysozyme by iodide ion. *Biochemistry* **1971**, *10*, 3254−3263.
(42) Albrecht, C.; Joseph, R. Lakowicz: Principles of fluorescence spectroscopy, 3rd Edition. *Anal. Bioanal. Chem.* **2008**, *390*, 1223−1224.
(43) Rajendran, D.; Chandrasekaran, N.; Waychal, Y.; Mukherjee, A. Nanoplastics alter the conformation and activity of human serum albumin. *NanoImpact* **2022**, *27*, 100412.
(44) Rajendran, D.; Chandrasekaran, N. Molecular Interaction of Functionalized Nanoplastics with Human Hemoglobin. *J. Fluoresc.* **2023**, *33*, 2257.
(45) Makowska, J.; Wiczk, W.; Kasprzykowski, F.; Chmurzyński, L.; Bagińska, K.; Bagińska, B.; et al. Conformational studies of alanine-rich peptide using CD and FTIR spectroscopy. *J. Pept. Sci.* **2008**, *14*, 283−289.
(46) Li, Y.; He, W. Y.; Dong, Y. M.; Sheng, F.; Hu, Z. Human serum albumin interaction with formononetin studied using fluorescence anisotropy, FT-IR spectroscopy, and molecular modeling methods. *Bioorg. Med. Chem.* **2006**, *14*, 1431−1436.
(47) De Meutter, J.; Goormaghtigh, E. Evaluation of protein secondary structure from FTIR spectra improved after partial deuteration. *Eur. Biophys. J.* **2021**, *50*, 613−628.
(48) Fujiwara, K.; Toda, H.; Ikeguchi, M. Dependence of α-helical and β-sheet amino acid propensities on the overall protein fold type. *BMC Struct. Biol.* **2012**, *12*, 18.
(49) Sangster, A.; Hodson, M.; Tubb, H. Silicon deposition in higher plants. *Stud. Plant Sci.* **2001**, *8*, 85−113.

https://doi.org/10.1021/acsomega.4c07974
ACS Omega 2025, 10, 10866−10877

(50) Roberts, N. B. Review article: Human pepsins - Their multiplicity, function and role in reflux disease. *Aliment. Pharmacol. Ther.* **2006**, *24*, 2−9.
(51) Vergnolle, N. Protease inhibition as new therapeutic strategy for GI diseases. *Gut* **2016**, *65*, 1215−1224.
(52) By, R.; Modification, C. *Modulation of Enzyme Activity*, 2007; Vol. *2*, pp 1−11.
(53) Palmer, T.; Bonner, P. L. Enzyme Inhibition. *Enzymes* **2011**, 126−152.
(54) Roskoski, R. Modulation of Enzyme Activity. *XPharm. Compr Pharmacol Ref* **2007**, *1*−*11*, 1.
(55) Miyanaga, K.; Unno, H. Reaction Kinetics and Stoichiometry. *Compr. Biotechnol.* **2011**, *2*, 33−46.
(56) Pang, G.; Xie, J.; Chen, Q.; Hu, Z. How functional foods play critical roles in human health. *Food Sci. Hum. Wellness* **2012**, *1*, 26−60.
(57) Rajendran, D.; Chandrasekaran, N. Unveiling the Modification of Esterase-like Activity of Serum Albumin by Nanoplastics and Their Cocontaminants. *ACS Omega* **2023**, *8*, 43719−43731.

https://doi.org/10.1021/acsomega.4c07974
ACS Omega 2025, 10, 10866−10877